NJC

PAPER

N-heterocyclic carbene supported Au(I) and Au(III) complexes: a comparison of cytotoxicities†

Cite this: DOI: 10.1039/c3nj01463k

Joydev Dinda,‡*[a] Tapastaru Samanta,[a] Abhishek Nandy,[b] Krishna Das Saha,[b] Saikat Kumar Seth,[c] Shymal Kumar Chattopadhyay[d] and Christopher W. Bielawski[e]

Received (in Victoria, Australia) 26th November 2013, Accepted 7th January 2014

DOI: 10.1039/c3nj01463k

www.rsc.org/njc

The N-heterocyclic carbene (NHC) precursor 2-pyridin-2-yl-2*H*-imidazo[1,5-*a*]pyridin-4-ylium hexafluorophosphate (**1**·**HPF$_6$**) was used to synthesize various Ag and Au complexes, including [Ag(**1**)$_2$][PF$_6$] (**2**), [Au(**1**)$_2$][PF$_6$] (**3**) and [Au(**1**)Cl$_3$] (**4**). The structure of the silver(I) complex **2** was established *via* NMR spectroscopy, mass spectrometry and single crystal X-ray crystallography. The gold(I)–NHC complex **3** was synthesized *via* transmetallation of the aforementioned silver complex and characterized using various spectroscopic methods. Treatment of **3** with Au(SMe$_2$)Cl afforded **4**, ostensibly *via* a disproportionation process. Close inspection of the solid state structure of **2** revealed that the Ag(I) center adopted a linear geometry; in contrast, a square planar geometry was observed for the solid structure of **4**. The cytotoxicities of the gold complexes **3** and **4** were tested *in vitro* against Human colorectal carcinoma (HCT 116), Human hepatocellular carcinoma (HepG2), Human breast adenocarcinoma (MCF-7) and Murine melanoma (B16F10). The measured IC$_{50}$ values showed that the Au(I) complex **3** was more potent than the Au(III) complex **4** as well as cisplatin.

Introduction

N-heterocyclic carbenes (NHCs) often serve as neutral σ-donating ligands for a broad range of transition metals, many of which are catalytically active.[1–4] Although NHCs display coordination chemistry that is similar to the phosphines, the former are relatively strong σ-donors and weak π-acceptors.[5,6] Over the past decade, a broad range of silver(I) and gold(I) complexes supported by NHCs have been synthesized and studied for their rich structural features,[7] potentially useful photophysical properties,[8,9] and as intermediates for accessing other types of metal complexes supported by NHCs.[10] Although the biomedical applications of coinage metal–NHC complexes have been summarized,[11] various Ag(I)–NHC complexes have been shown to be potent agents against drug resistant pathogens.[11–14] Such silver complexes seem to display a mode of action which involves the release of Ag^+ ions that enter cell membranes and disrupt cell functions. A drawback of many silver containing drugs, however, is that, they quickly lose their potency due to a rapid release of the Ag^+ ions. To overcome this obstacle, promising strategies have capitalized on the relatively strong Ag–$C_{carbene}$ bond. For example, Young described a series of Ag–NHC complexes derived from 4,5-dichloro-1*H*-imidazole and showed that these complexes exhibit cytotoxic activity against ovarian (OVCAR-3) and breast (MB157) cancer cells *in vitro*.[14] Similarly, a library of cationic silver–NHC complexes developed by the Willans group were found to exhibit cytotoxicities that were comparable to cisplatin against the adenocarcinomas MCF7 and DLD1.[12b] Gautier and Morel also reported Ag–NHC complexes which exhibited cytotoxicities that were greater than cisplatin against various cell lines.[12c]

While many metal-based anticancer drugs are based on platinum (*e.g.*, cisplatin and carboplatin), these compounds often suffer from a number of limitations, including neurotoxicity, nephrotoxicity and resistance to some cancer cell lines.[15] As an alternative, the gold(I) phosphine complex auranofin, which was initially developed as an anti-rheumatic agent, was shown to have potential for use as an anticancer agent.[16] Unfortunately, auranofin is readily metabolized by natural thiols which significantly restricts its activity.[17] To increase the stability of gold complexes under biologically relevant conditions, attention has been directed toward the synthesis and study of complexes bearing NHC ligands.[18] Notably, during these studies, it was suggested that

[a] *School of Applied Science, "Applied Synthetic Chemical Research Laboratory", Haldia Institute of Technology, Purba Medinipur, Haldia-721657, West Bengal, India. E-mail: dindajoy@yahoo.com*
[b] *Cancer Biology and Inflammatory Disorder Division, CSIR-Indian Institute of Chemical Biology, Jadavpur, Kolkata-700032, West Bengal, India*
[c] *Department of Physics, M. G. Mahavidyalaya, Purba Medinipur, West Bengal 721425, India*
[d] *Department of Chemistry, Bengal Engineering and Science University, Shibpur, Howrah-711 103, West Bengal, India*
[e] *Department of Chemistry, University of Texas at Austin, 1 University Station, A1590, Austin, TX 78712, USA*

† CCDC 910111 and 900036. For crystallographic data in CIF or other electronic format see DOI: 10.1039/c3nj01463k

‡ Present address: Department of Chemistry, ITM University-Gwalior, Gwalior-474001, M.P., India.

the mode of apoptotic activity displayed by Au(I)–NHC complexes towards cancer cells could involve deactivation of the selenoenzyme thioredoxin reductase, which in turn causes oxidation of the thioredoxins.[19] Though many Au(I)–NHC complexes have been synthesized relatively less attention has been directed toward Au(III) analogues. Due to their enhanced electrophilicity, we reasoned that such Au(III) complexes may display enhanced activities under similar conditions.[14]

Herein the cytotoxicities of Au(I) and Au(III) complexes supported by a pyridine annulated imidazole-2-ylidene[20] were evaluated *in vitro* on a range of cell lines. The aforementioned complexes were synthesized *via* transmetallation from a Ag(I)–NHC complex *via* a disproportionation process that strictly avoided the use of noxious oxidants (*e.g.*, Cl_2 or Br_2).[21] In general, the Au(I) complex was found to be more cytotoxic than the analogous Au(III) complex as well as cisplatin.

Results and discussion

The salt 2-pyridin-2-yl-2*H*-imidazo[1,5-*a*]pyridin-4-ylium hexafluorophosphate (**1·HPF$_6$**) was synthesized *via* formylative cyclization of the corresponding Schiff base 2-pyridyl-*N*-(2-pyridine)-methylamine using standard conditions followed by anion metathesis with NH_4PF_6.[20] Treatment of Ag_2O with **1·HPF$_6$** afforded the Ag(I)–NHC complex **2** (Scheme 1), as determined by the absence of the diagnostic ^{1}H NMR signal associated with the imidazolium precursor (δ = 10.43 ppm (s); DMSO-d_6). In addition, the ^{1}H NMR spectrum recorded for **2** revealed two doublets in the range of 7.16–7.89 ppm, which were assigned to the two α-pyridine protons associated with the ligand. Although Ag–C coupling was not observed, a singlet was recorded at 170.60 ppm upon ^{13}C NMR spectroscopic analysis of a solution of **2** and attributed to a carbene nucleus. The formation of a complex coordinated to two ligands was supported by mass spectrometry, which revealed a signal consistent with a $[Ag(\mathbf{1})_2]^+$ ion (*m*/*z* = 497.06). Additional support for the structure of **2** was obtained *via* single crystal X-ray crystallography. As shown in Fig. 1, the solid state structure of **2** revealed that two carbene centers were coordinated to the Ag center with an average

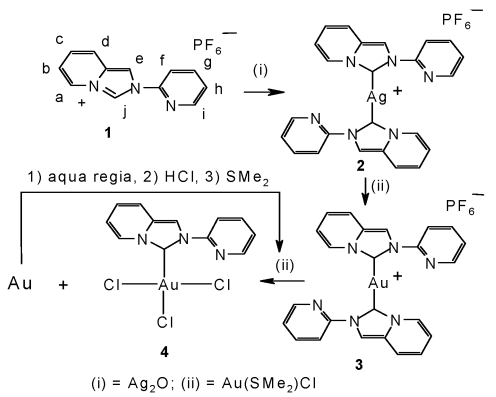

Scheme 1 Synthesis of various NHC complexes. The letters surrounding the structure of **1** refer to the NMR assignments; see the Experimental section.

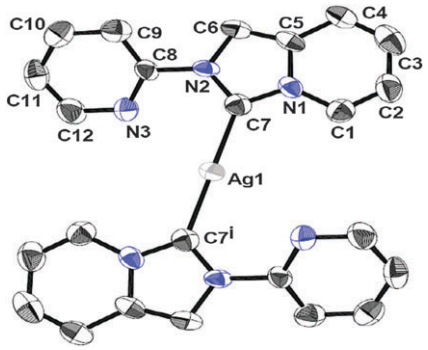

Fig. 1 ORTEP diagram of **2** shown at the 50% probability level. The H atoms and PF_6 anions have been removed for clarity. C(7^i) denotes the equivalent position of C(7) where (symmetry code for i = $-x$ + 1, $-y$ + 1, $-z$). Bond lengths (Å) and angles (°): Ag(1)–C(7) = 2.086(7); N(1)–C(7) = 1.362(10); N(2)–C(7) = 1.348(10); C(7)–Ag(1)–C7^i = 180.0(3); N(1)–C(7)–N(2) = 103.2(6); N(2)–C(6)–C(5) = 105.9(7).

Ag(I)–C distance of 2.086(7) Å. Additional crystallographic details are summarized in Table 1 and discussed below.

The commercially available complex Au(SMe$_2$)Cl was successfully transmetalled[10] with **2** (formed *in situ* using the aforementioned method) to afford Au(I)–NHC (**3**).[21] Complex **3** displayed a ^{13}C NMR signal at 172.60 ppm and a *m*/*z* signal at 587.12, consistent with a $[Au(\mathbf{1})_2]^+$ ion. Following a protocol previously reported by our group, the Au(III)–NHC complex **4** was synthesized using **3** and Au(SMe$_2$)Cl as a precursor.[21] Upon stirring a colorless acetonitrile solution of the Au(I)–NHC complex (**3**) and Au(SMe$_2$)Cl at room temperature for 5–6 h, an orange/yellow color formed along with the appearance of a yellow precipitate and Au(0); the latter may be isolated and reconverted to Au(SMe$_2$)Cl. After separation and purification, the yellow

Table 1 Summary of key crystal data for **2** and **4**

	Complex (**2**)	Complex (**4**)
Empirical formula	$C_{24}H_{18}N_6F_{12}P_2Ag$	$C_{12}H_9N_3AuCl_3$
Formula weight	788.25	498.54
Temperature (K)	150(2)	293(2)
Wavelength (Å)	0.71073	0.71073
Crystal system	Monoclinic	Triclinic
Unit cell dimensions		
a (Å)	3.8994(4)	7.8238(18)
b (Å)	15.6005(15)	9.795(2)
c (Å)	21.254(2)	10.093(2)
α (°)	90	112.116(5)
β (°)	93.240(2)	95.677(5)
γ (°)	90	97.329(6)
Volume	1290.9(2)	701.6(3)
Z	2	2
Calcd density (g cm^{-3})	2.028	2.360
Absorption coefficient	1.023	11.042
F(000)	778	464
Crystal size (mm)	0.17 × 0.11 × 0.08	0.09 × 0.14 × 0.21
θ range (°)	1.62–25.00	1.50–25.0
Reflections collected/ unique data/*R*(int)	11 831/2285/0.0409	6447/2463/0.0516
Observed data/parameters	2285/205	2463/172
Goodness-of-fit on F^2	1.073	1.114
Final *R* indices [$I > 2\sigma(I)$]	R_1 = 0.0741, wR_2 = 0.2130	R_1 = 0.0389, wR_2 = 0.0987
R indices (all data)	R_1 = 0.0823, wR_2 = 0.2202	R_1 = 0.0475, wR_2 = 0.1060

product was analyzed by NMR spectroscopy. Although the ^{1}H NMR spectrum of the isolated solid was similar to that recorded for complex **3**, the former displayed a relatively upfield ^{13}C NMR signal at δ = 159.65 ppm, which was subsequently assigned to a $C_{carbene}$ atom coordinated to a Au(III) center. For comparison, the ^{13}C NMR resonance observed for the $C_{carbene}$ atom in the isolated material was slightly downfield with respect to the NCHN signal recorded for the parent imidazolium salt (148.70 ppm)[20] but consistent with analogous signals displayed by [AuX$_3$(NHC)] complexes bearing imidazolin-2-ylidene or imidazolidin-2-ylidene ligands.[10,22,23] The isolated material was further examined by mass spectrometry, which revealed signals consistent with [Au(**1**)Cl$_2$]$^+$ (*m*/*z* of 463) and [Au(**1**)Cl]$^{2+}$ (*m*/*z* of 427.5). Collectively, these results, combined with a detailed X-ray crystallographic study (see Fig. 2 and accompanying discussion below), indicated that the structure of the isolated material was in agreement with that of **4** shown in Scheme 1.

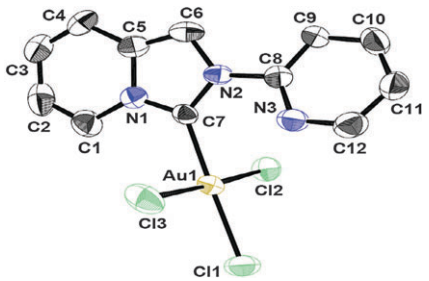

Fig. 2 ORTEP diagram of **4** shown at the 50% probability level. The H atoms have been removed for clarity. Bond lengths (Å) and angles (°): Au(1)–C(7) = 2.005(9); Au(1)–Cl(2) = 2.289(3); Au(1)–Cl(3) = 2.292(3); Au(1)–Cl(1) = 2.301(3); N(1)–C(7) = 1.328(12); N(2)–C(7) = 1.352(12); C(7)–Au(1)–Cl(2) = 88.7(3); C(7)–Au(1)–Cl(3) = 88.4(3); Cl(2)–Au(1)–Cl(3) = 176.45(10); C(7)–Au(1)–Cl(1) = 178.2(3); Cl(2)–Au(1)–Cl(1) = 91.50(11); Cl(3)–Au(1)–Cl(1) = 91.52(12); N(1)–C(7)–N(2) = 106.8(8).

Single crystals suitable for X-ray diffraction were grown from slow diffusion of diethyl ether into a DMSO solution saturated with **2**. As shown in Fig. 1, a linear (180.0(3)°) $C_{carbene}$–Ag(I)–$C_{carbene}$ bonding arrangement was observed. Moreover, the Ag–C distance (2.086(7) Å) was consistent with those measured in the solid state structures of other Ag–NHC complexes[7,8] and within the sum of van der Waals radii of silver and carbon nuclei (2.111 Å). The N(1)–C(7)–N(2) bond angle was measured to be 103.2(6)°, which was more acute than that reported for a Hg(II)–NHC complex containing the same ligand (105.6(4)°).[19] Close inspection of the solid state structure of **2** indicated that the pendant pyridyl rings were not coordinated to the metal center, similar to an arrangement observed for the aforementioned Hg(II)–NHC complex.[20] The solid state structure also revealed several C–H···F interactions with measured distances of 2.48 to 2.51 Å, respectively. As shown in Scheme 2, H-bonds were formed with the PF_6 groups and ultimately resulted in the formation of a 2-D network with stair-like, wave-like and ribbon-like structures (Scheme 3).

To gain additional insight into the coordination chemistry of complex **4**, single crystals were grown by slow diffusion of Et_2O into a concentrated acetonitrile solution of the complex and characterized by X-ray diffraction; the corresponding structure is shown in Fig. 2 and key crystallographic parameters are listed in Table 1. As expected for a metal complex in a square planar environment, nearly linear C(7)–Au(1)–Cl(1) and Cl(2)–Au(1)–Cl(3) angles (178.2(3) and 176.45(10)°) and perpendicular C(7)–Au(1)–Cl(2), C(7)–Au(1)–Cl(3), Cl(2)–Au(1)–Cl(1) and Cl(3)–Au(1)–Cl(1) angles (88.4(3)–91.52(12)°) were measured. While the Au(1)–C(7) distance (2.005(9) Å) was measured to be similar in length to analogous bond distances observed in gold(III) complexes of the type [AuBr$_3$(NHC)] (NHC = imidazolin-2-

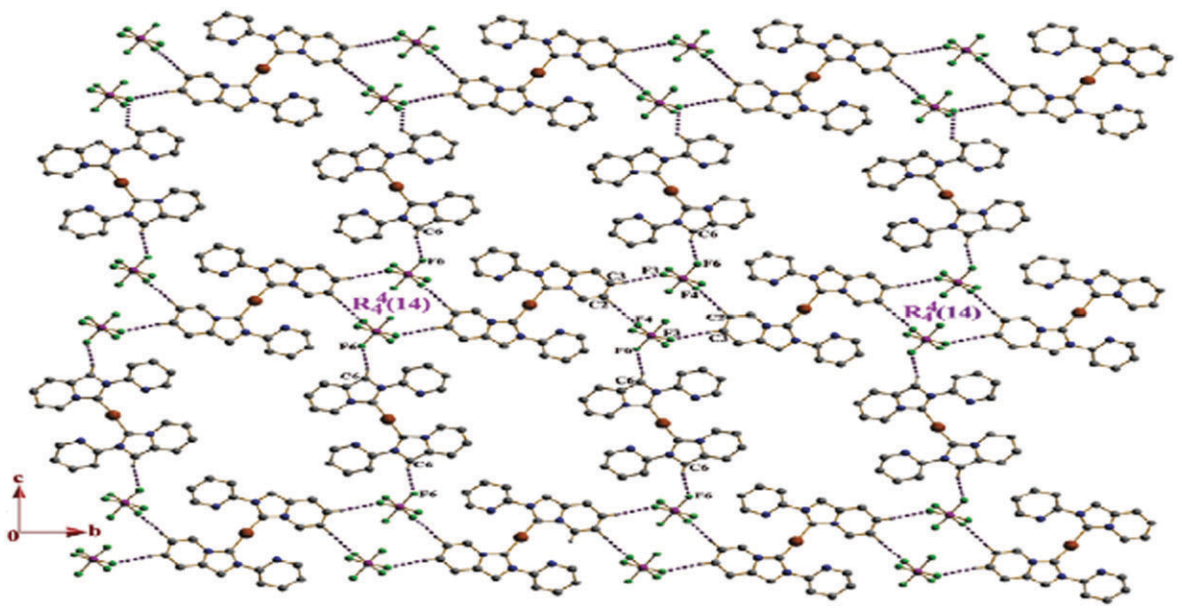

Scheme 2 Depiction of the two-dimensional supramolecular network formed *via* strong complementary C–H···F hydrogen bonds in the solid state structure of **2**. In addition, an interconnected 2D chain formed through self-complementary H bonds resulted in R_4^4 (14) dimeric rings. H atoms not involved in hydrogen bonding have been omitted for clarity.

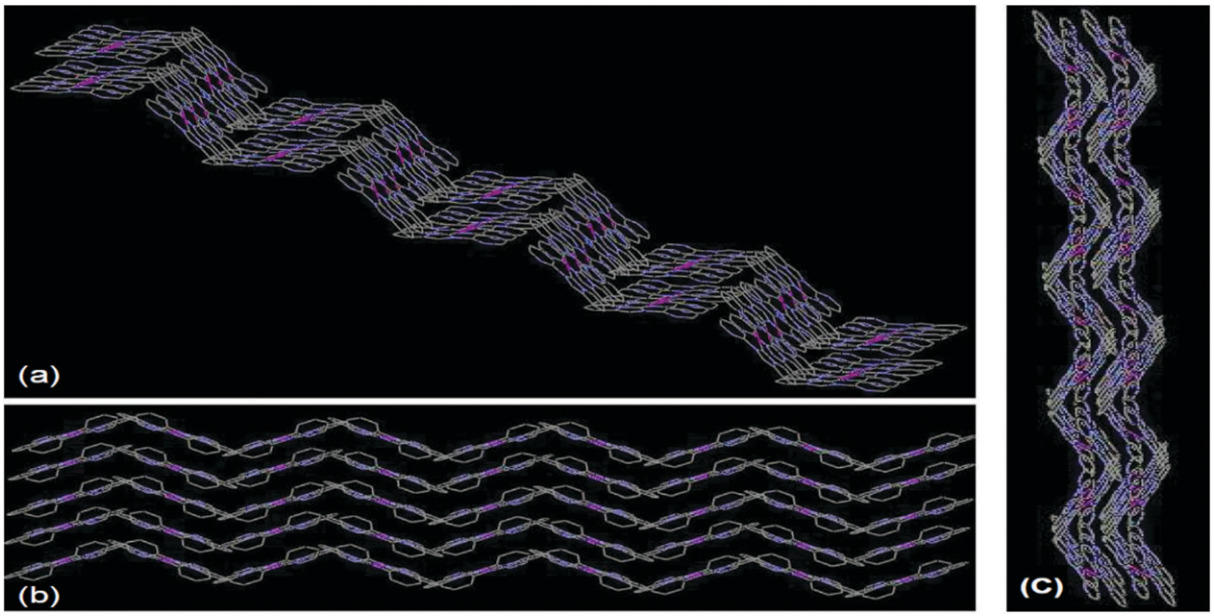

Scheme 3 Depiction of (a) stair-like, (b) wave-like and (c) ribbon-like structures observed in the solid state structure of **2**.

ylidene or imidazolidin-2-ylidene),[22] the N–$C_{carbene}$–N bond angle **4** (106.8(8)°) was slightly wider than the equivalent angle found in an analogous Au(I) complex.[19] Due to the strong donating ability of the NHC, the Au–Cl bond *trans* to the ligand in **4** was longer than the *cis* Au–Cl bonds (*cf.*, 2.301(3) Å *vs.* 2.289(3)–2.292(3) Å, respectively).[14,21–23] Driven by the formation of C–H···Cl and π–π bonding interactions, the complex formed a 1-D polymer in the solid state (see Scheme 4).

With **3** and **4** in hand, the cytotoxicities of these complexes toward the Human colorectal carcinoma (HCT 116), Human hepatocellular carcinoma (HepG2), Human breast adenocarcinoma (MCF-7) and Murine melanoma (B16F10) cell lines were examined; representative data obtained for the B16F10 cell line are summarized in Fig. 3. As summarized in Table 2, the IC_{50} values measured for **3** were found to be nearly three times lower than cisplatin and generally lower than gold(III) complex **4**. Thus, while the Au(I) complex **3** exhibited higher cytotoxicities than the Au(III) complex **4** for nearly all of cell lines tested, both of the aforementioned gold complexes exhibited higher cytotoxicities than cisplatin. Collectively, these results were remarkable as previous Cl–Au(I)–NHC complexes were found to display cytotoxicities comparable to that of cisplatin.[24]

As shown in Fig. 4, a series of microscopic analyses were performed in order to distinguish between control and treated cells undergoing apoptosis. B16F10 cells treated with complexes **3** or **4** at 10 μM initial concentrations for 24 h underwent a morphological change. Likewise, cells treated with **3** or **4** followed by staining with 4,6-diamidino-2-phenylindole showed bright, fragmented nuclei under a fluorescence microscope when compared to untreated cells. In parallel, the aforementioned cells were exposed to FITC labeled Annexin V and monitored by fluorescence activated cell sorting analysis.[25] B16F10 cells treated with the complexes **3** or **4** (10 μM initial concentration) showed apoptotic cell populations of 75.02% and 47.21%, respectively, which were significantly higher than the 0.45% measured in the control experiment after 24 h (Fig. 5). Collectively, these results were consistent with the hallmarks of apoptosis.[26]

To gain insight into the apoptosis mechanism, a series of colorimetric assays were performed according to the manufacturer's instructions for the detection of caspase-3, caspase-8 and caspase-9 activity. As summarized in Fig. 6, the activation

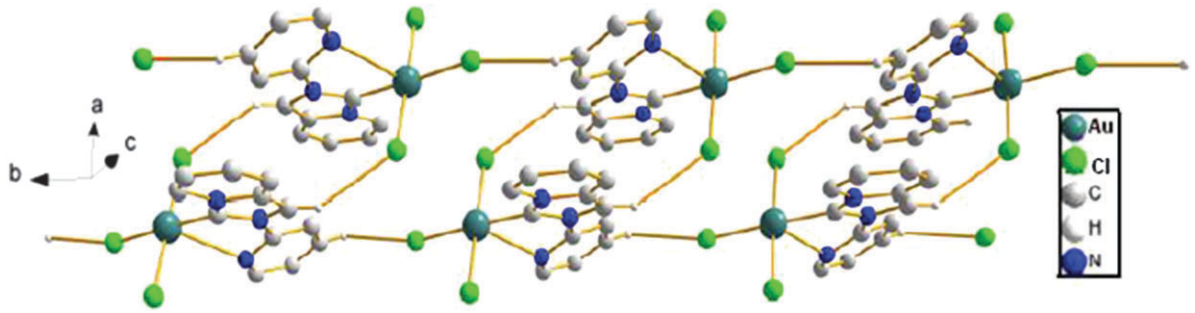

Scheme 4 Depiction of a 1-D polymer formed through C–H···Cl bonding observed in the solid state structure of **4**.

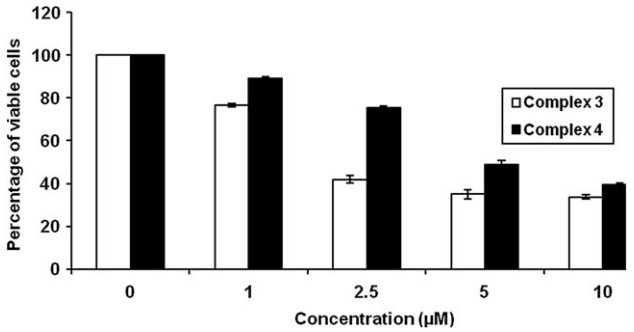

Fig. 3 Summary of a MTT cell viability assay where 5×10^3 cells were treated with varying concentrations [0–10 μM] of complexes **3** or **4** for 24 h followed by analysis. Mean values ± standard deviation are reported.

Table 2 Summary of IC_{50} values (μM) against B16F10, HCT 116, HepG2 and MCF-7 cell lines

Cell line	3	4	Cisplatin
B16F10	2.13 ± 0.08	4.87 ± 0.04	7.39 ± 0.31
HCT-116	2.25 ± 0.14	4.73 ± 0.34	8.51 ± 0.25
HepG2	2.44 ± 0.35	5.12 ± 0.26	6.50 ± 0.38
MCF7	2.15 ± 0.37	5.34 ± 0.32	10.52 ± 0.30

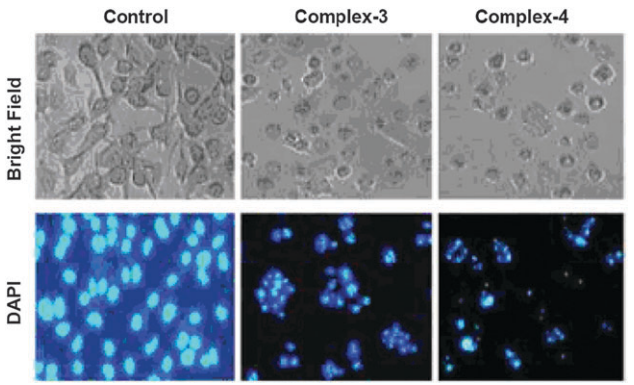

Fig. 4 (top) Morphological and (bottom) nuclear changes observed in B16F10 cells after treatment with 10 μM of complex **3** or **4** for 24 h using light microscope or under a fluorescence microscope after staining with DAPI, respectively.

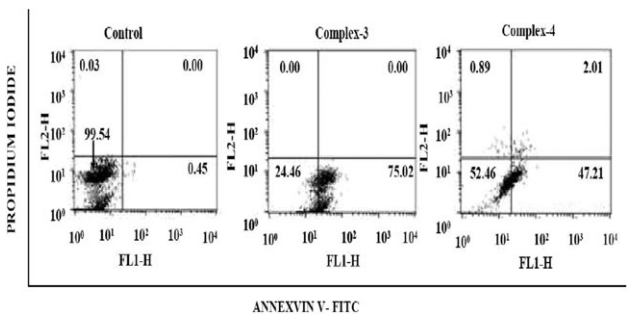

Fig. 5 Summary of flow cytometry studies of the B16F10 cells following treatment with **3** or **4** at 10 μM for 24 h.

of caspase-9 and caspase-3 was observed in the B16F10 cells treated with Au(I) complex **3**, a result consistent with the involvement of an intrinsic apoptotic pathway.[26]

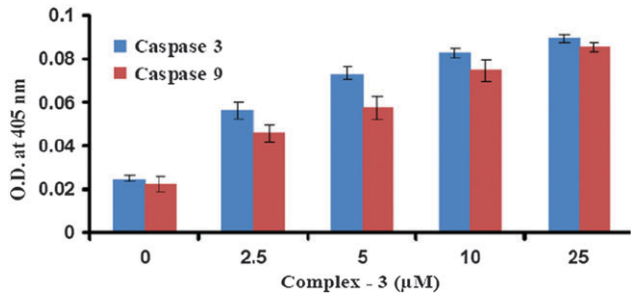

Fig. 6 Caspase-3 and Caspase-9 activity following treatment of B16F10 cells with complex **3** ($[\mathbf{3}]_0$ = 0, 2.5, 5, 10 and 25 μM) for 24 h.

Conclusions

In conclusion, we have synthesized two novel gold complexes *via* transmetallation of a Ag precursor. According to the solid-state structures, a linear coordination geometry of Ag(I)–NHC, **2** has been established by X-ray diffraction studies; whereas the Au(III)–NHC complex (**4**) adopts the square planar geometry. The complex **2** forms a beautiful stair-like structure. Following characterization, the cytotoxicities of the aforementioned complexes were explored in four cancer cell lines. In one line, *Murine* melanoma (B16F10), the Au(I) complex **3** was found to display higher cytotoxicity than the Au(III) analogue **4** as well as cisplatin. We believe these results will guide the development of other Au-based compounds, particularly those intended for biological applications.

Experimental section

General procedures

The following reagents were purchased from Sigma Aldrich, UK and used without additional purification: Ag_2O, NH_4PF_6, pyridine-2-carboxaldehyde, and 2-aminopyridine. $Au(SMe_2)Cl$ was prepared according to a previously reported procedure.[27] All manipulations were carried out under an ambient atmosphere. NMR spectra were recorded on a Bruker NMR spectrometer at 25 °C using tetramethylsilane as an internal standard (^1H: 400 MHz; ^{13}C: 100 MHz). Cells were obtained from National Centre for Cell Science, Pune. Dulbecco's Modified Eagle Medium (DMEM), fetal bovine serum (FBS), penicillin streptomycin neomycin (PSN) antibiotic, trysin and ethylenediaminetetraacetic acid (EDTA) were obtained from Gibco BRL (Grand Island, NY, USA). Tissue culture plastic wares were obtained from NUNC (Rokskidle, Denmark). DAPI (4,6-diamidino-2-phenylindole dihydrochloride) was obtained from Invitrogen, CA. 3-(4,5-Dimethylthiazol-2-yl)-2,5-diphenyltetrazolium bromide (MTT) was obtained from SRL, India. The caspase-3, caspase-8 and caspase-9 assay kits were obtained from Biovision (Biovision Research Products, USA).

General syntheses

Synthesis of 1·HPF$_6$. Using a modification[20] of a previously reported procedure, 2-pyridyl-*N*-(2-pyridyl) methylamine (1.0 g,

5.5 mmol), 2 drops of formic acid, 0.5 mL triethylorthoformate, crushed 91% paraformaldehyde powder (0.180 g, 5.5 mmol) and 20 mL dioxane were combined to obtained 1.39 g (72%) of the desired compound. Spectral data were in accordance with previously reported values.[20]

Synthesis of 2. The salt **1·HPF$_6$** (250 mg, 0.73 mmol) and silver oxide (85 mg, 0.37 mmol) were combined in dry acetonitrile and stirred at room for 4 h. The solution was filtered through a plug of celite to remove the residual Ag_2O and the solvent was removed under reduced pressure. The desired material was obtained by dissolving 210 mg of **2** in 15 mL of CH_3CN followed by vapor diffusing 5 mL of Et_2O into the aforementioned solution and isolated in 86% yield (203 mg, 0.32 mmol). ^{1}H NMR (DMSO-d_6, 300 MHz, 25 °C): δ 8.66 (d, J = 3.0 Hz, 1H, H^a), 8.59 (s, 1H, H^e), 8.44 (d, J = 7.6 Hz, 1H, H^i), 8.24 (d, J = 7.6 Hz, 1H, H^d), 8.09 (t, J = 7.7 Hz, 1H, H^c), 7.71 (d, J = 9.0 Hz, 1H, H^f), 7.59 (m, 1H, H^h), 7.14 (m, 1H, H^b), 6.98 (t, J = 7.8 Hz, 1H, H^g). ^{13}C NMR (DMSO-d_6, 100 MHz, 25 °C) δ 170.61 (N*C*N), 148.94 (py-C$_a$), 147.27 (py-C$_i$), 138.44 (im-C$_e$), 129.58 (py-C$_m$), 127.47 (py-C$_k$), 123.18 (py-C$_d$), 122.30 (py-C$_f$), 116.57 (py-C$_c$), 115.02 (py-C$_h$), 113.72 (py-C$_b$), 109.40 (py-C$_g$). Anal. calcd for $C_{24}H_{18}N_6AgPF_6$: C, 44.79; H, 2.79; N, 13.06%. Found: C, 44.68; H, 2.76; N, 12.97%.

Synthesis of 3. The salt **1·HPF$_6$** (250 mg, 0.73 mmol) and silver oxide (85 mg, 0.37 mmol) were combined in dry acetonitrile and stirred at room temperature for 4 h. The resulting solution was filtered through a plug of celite to remove the unreacted Ag_2O and the residual solvent was removed under reduced pressure. A concentrated acetonitrile solution of $Au(SMe_2)Cl$ (108 mg, 0.37 mmol) was then added dropwise to the silver containing mixture. An immediate white precipitate, presumably AgCl, was formed and subsequently removed through filtration. Following drying of the resulting solid, the desired compound was obtained by dissolving 200 mg of **3** in 15 mL of CH_3CN followed by vapor diffusing 5 mL of Et_2O into the aforementioned solution and isolated in 70% yield (188 mg, 0.26 mmol). ^{1}H NMR (DMSO-d_6, 400 MHz, 25 °C): δ 8.78 (d, J = 3.0 Hz, 1H, H^a), 8.66 (s, 1H, H^e), 8.46 (d, J = 7.2 Hz, 1H, H^i), 8.25 (d, J = 1 Hz, 1H, H^d), 8.10 (t, J = 7.7 Hz, 1H, H^c), 7.72 (d, 1H, H^f), 7.60 (m, 1H, H^h), 7.15 (m, 1H, H^b), 7.08 (t, 1H, H^g). ^{13}C NMR (DMSO-d_6, 100 MHz, 25 °C): δ 172.60 (N*C*N), 149.94 (py-C$_a$), 147.57 (py-C$_i$), 138.46 (im-C$_e$), 129.60 (py-C$_m$), 127.49 (py-C$_k$), 123.18 (py-C$_d$), 122.32 (py-C$_f$), 116.57 (py-C$_c$), 115.05 (py-C$_h$), 113.74 (py-C$_b$), 109.41 (py-C$_g$). Anal. calcd for $C_{24}H_{18}N_6AuPF_6$: C, 39.34; H, 2.46; N, 11.48%. Found: C, 39.29; H, 2.47; N, 11.46%.

Synthesis of 4. After dissolving complex **3** (200 mg, 0.27 mmol) in acetonitrile (10 mL) at room temperature, $Au(SMe_2)Cl$ (160 mg, 0.54 mmol) was added and the resulting mixture was stirred for an additional 6 h. The colour of the solution turned yellow (from colourless) and was accompanied by the formation of a small amount of precipitate. The precipitate was presumed to be metallic gold and reused to synthesize $Au(SMe_2)Cl$. After filtration, the residual acetonitrile was removed under reduced pressure and at low temperature to obtain a yellow powder. The desired compound was obtained by dissolving 100 mg of 4 in 10 mL of CH_3CN followed by vapor diffusing 3 mL of Et_2O into the aforementioned solution and isolated in 60% yield (82 mg, 0.16 mmol) ^{1}H NMR (DMSO-d_6, 400 MHz, 25 °C): δ 9.10 (s, 1H, H^e), 8.82 (d, J = 7.2 Hz, 1H, H^a), 8.62 (d, J = 7.2 Hz, 1H, H^i), 8.17 (t, J = 7.4 Hz, 1H, H^c), 8.06 (d, J = 7.2 Hz, 1H, H^d), 7.89 (d, J = 7.2 Hz, 1H, H^f), 7.62 (m, 1H, H^h), 7.31 (t, J = 9.0 Hz, 1H, H^b), 7.21 (t, 1H, H^g). ^{13}C NMR (DMSO-d_6, 100 MHz, 25 °C):δ 159.65 (N*C*N), 146.26 (py-C$_a$), 141.35 (py-C$_i$), 130.65 (im-C$_e$), 126.06 (py-C$_m$), 125.92 (py-C$_k$), 125.90 (py-C$_d$), 125.73 (py-C$_f$), 124.96 (py-C$_c$), 124.79 (py-C$_h$), 119.38 (py-C$_b$), 110.38 (py-C$_g$). Anal. calcd for $C_{12}H_9N_3AuCl_3$: C, 28.88; H, 1.80; N, 8.43%. Found: C, 28.79; H, 1.82; N, 8.39%.

X-ray crystallography. Single crystals suitable for data collection were grown from DMSO/Et_2O and CH_3CN/Et_2O for **2** and **4**, respectively. The crystal data and details of the data collections are given in Table 1. X-ray data were collected on a CCD diffractometer (graphite monochromated MoKα radiation, λ = 0.71073 Å). The structures were solved by direct methods and refined on F^2 using all reflections with SHELX-97.[28] The non-hydrogen atoms were refined anisotropically. Hydrogen atoms which were not bound to imidazolium-C2 atoms were placed in calculated positions and assigned an isotropic displacement parameter of 0.08 Å. CCDC 910111 (**2**) and 900036 (**4**).

Cytotoxicity studies

Cell Culture Studies. Human colorectal carcinoma (HCT 116), Human hepatocellular carcinoma (HepG2), Human breast adenocarcinoma (MCF-7) and Murine melanoma (B16F10) cell lines were cultured in DMEM supplemented with 10% fetal bovine serum (FBS) and 1% antibiotic (PSN) at 37 °C in a humidified atmosphere under 5% CO_2. After 75–80% confluency, 5h3 cells were harvested with 0.025% trypsin and 0.52 mM EDTA in phosphate buffered saline (PBS), and seeded at a desired density to allow equilibration one day before the start of experiments described below.

MTT Assays. MTT assays[29] were performed to evaluate viability of Human colorectal carcinoma (HCT116), Human hepatocellular carcinoma (HepG2), Human breast adenocarcinoma (MCF-7) and Murine melanoma (B16F10) cell lines following treatment with **3** or **4**. The cells were plated in 96 well plates and treated with different concentrations (0, 1, 2.5, 5, and 10 μM) of complexes **3** or **4** for 24 h. Four hours after the addition of MTT, the cells were lysed and formazan was solubilized with acidic isopropanol. The absorbance of the solution was then measured at 595 nm using an ELISA reader. All the experiments were performed in triplicate.

Microscopy. To determine morphological changes, B16F10 cells were grown in 24 well plates, untreated (control) or treated with 10 μM of complex **3** or **4**, respectively, for 24 h, and then washed twice with PBS prior to examination under a light microscope. Morphological changes were observed in an inverted phase using a contrast microscope (Model: OLYMPUS IX 70, Olympus Optical Co. Ltd., Sibuya-ku, Tokyo, Japan). For the detection of chromatin condensation and DNA fragmentation, treated B16F10 cells were stained with 10 μg mL^{-1} of DAPI and visualized using a fluorescence microscope (Model: OLYMPUS IX70, Olympus Optical Co.

Ltd., Shibuya-ku, Tokyo, Japan). Images were acquired with an excitation wavelength at 488 nm and emission at 550 nm.

Assay using Annexin-V and propidium iodide. Apoptosis was assayed through the use of an Annexin-V FITC apoptosis detection kit (Calbiochem, CA, USA). Briefly, B16F10 cells were treated with 10 μM of complex **3** or **4**, respectively, for 24 h, and then washed and stained with PI and Annexin-V-FITC in accordance with the manufacturer's instructions. The percentages of live, apoptotic and necrotic cells were determined by flow cytometry (Beckton Dickinson, San Jose, CA, USA). Data from 10^4 cells were analyzed for each sample.

Caspase-3 and Caspase-9 sssay. Caspase-3 and Caspase-9 activities were quantified using commercially available Caspase-3/CPP32 and FLICE/Caspase-9 Colorimetric Assay kits (BioVision Research Products, Mountain View, CA), respectively. The assays were performed on the B16F10 cells (1×10^4) treated with **3** ($[\mathbf{3}]_0$ = 0, 1, 2.5, 5, and 10 μM) for 24 h according to the manufacturer's instructions using DEVD-*p*NA and LEDH-*p*NA as substrates for Caspase-3 and Caspase-9, respectively. Caspase activity was spectrophotometrically detected at 405 nm using an ELISA reader (Model: Emax, Molecular device, USA).

Acknowledgements

We are thankful to Prof. Anindyakishore Bhowmik, the former principal Bajkul Milani Mahavidyalaya and the Department of Science and Technology, DST, India, for financial support under the 'SERC FAST TRACK' Young Scientist Scheme' (SR/FT/CS-046/2009). CWB is grateful to the NSF (CHE-1266323) for support.

References

1 E. Peris and R. H. Crabtree, *Coord. Chem. Rev.*, 2004, **248**, 2239–2246.
2 C. M. Crudden and D. P. Allen, *Coord. Chem. Rev.*, 2004, **248**, 2247–2273.
3 A. G. Tennyson, V. M. Lynch and C. W. Bielawski, *J. Am. Chem. Soc.*, 2010, **132**, 9420–9429.
4 J. R. Miecznikowski, S. Gruendemann, M. Albrecht, C. Megret, E. Clot, J. W. Faller, O. Eisenstein and R. H. Crabtree, *Dalton Trans.*, 2003, 831–838.
5 R. Tonner, G. Heydenrych and G. Frenking, *Chem.–Asian J.*, 2007, **2**, 1555–1567.
6 F. E. Hahn and M. C. Jahnke, *Angew. Chem., Int. Ed.*, 2008, **47**, 3122–3172.
7 T. H. Hsu, J. J. Naidu, B. J. Yang, M. Y. Jang and I. J. Lin, *Inorg. Chem.*, 2012, **51**, 98–108.
8 A. L. Chow, M. H. So, W. Lu, N. Zhu and C. M. Che, *Chem.–Asian J.*, 2011, **6**, 544–553.
9 J. T. Price, N. D. Jones and P. J. Ragogna, *Inorg. Chem.*, 2012, **51**, 6776–6783.
10 H. M. J. Wang and I. J. B. Lin, *Organometallics*, 1998, **17**, 972–975.
11 (*a*) W. Liu and R. Gust, *Chem. Soc. Rev.*, 2013, **42**, 755–773; (*b*) F. Cisnetti and A. Gautier, *Angew. Chem., Int. Ed.*, 2013, **52**, 11976–11978; (*c*) L. Oehninger, R. Rubbiani and I. Ott, *Dalton Trans.*, 2013, **42**, 3269–3284; (*d*) A. Gautier and F. Cisnetti, *Metallomics*, 2012, **4**, 23–32.
12 (*a*) C.-H. Wang, W.-C. Shih, H. C. Chang, Y.-Y. Kuo, W.-C. Hung, T.-G. Ong and W.-S. Li, *J. Med. Chem.*, 2011, **54**, 5245–5249; (*b*) D. C. Monteiro, R. M. Phillips, B. D. Crossley, J. Fielden and C. E. Willans, *Dalton Trans.*, 2012, **41**, 3720–3725; (*c*) M. L. Teyssot, A. S. Jarrousse, M. Manin, A. Chevry, S. Roche, F. Norre, C. Beaudoin, L. Morel, D. Boyer, R. Mahiou and A. Gautier, *Dalton Trans.*, 2009, 6894–6902.
13 C. Topf, C. Hirtenlehner, M. Zabel, M. List, M. Fleck and U. Monkowius, *Organometallics*, 2011, **30**, 2755–2764.
14 (*a*) G. Roymahapatra, S. M. Mandal, W. F. Porto, T. Samanta, S. Giri, J. Dinda, O. L. Franco and P. K. Chattaraj, *Curr. Med. Chem.*, 2012, **19**, 4184–4193; (*b*) J. C. Garrison and W. J. Youngs, *Chem. Rev.*, 2005, **105**, 3978–4008.
15 S. J. Berners-Price, *Angew. Chem., Int. Ed.*, 2011, **50**, 804–805.
16 N. H. Kim, H. J. Park, M. K. Oh and I. S. Kim, *BMB Rep.*, 2013, **46**, 59–64.
17 C. F. Shaw III, *Chem. Rev.*, 1999, **99**, 2589–2600.
18 W. Liu, K. Bensdorf, M. Proetto, U. Abram, A. Hagenbach and R. Gust, *J. Med. Chem.*, 2011, **54**, 8605–8615.
19 (*a*) E. Schuh, C. Pflüger, A. Citta, A. Folda, M. P. Rigobello, A. Bindoli, A. Casini and F. Mohr, *J. Med. Chem.*, 2012, **55**, 5518–5528; (*b*) T. Zou, C. T. Lum, S. S.-Y. Chui and C.-M. Che, *Angew. Chem., Int. Ed.*, 2013, **52**, 2930–2933.
20 T. Samanta, B. K. Rana, G. Roymahapatra, S. Giri, P. Mitra, R. Pallepogu, P. K. Chattaraj and J. Dinda, *Inorg. Chim. Acta*, 2011, **375**, 271–279.
21 J. Dinda, S. D. Adhikary, S. K. Seth and A. Mahapatra, *New J. Chem.*, 2013, **37**, 431–438.
22 (*a*) P. de Frémont, R. Singh, E. D. Stevens, J. L. Petersen and S. P. Nolan, *Organometallics*, 2007, **26**, 1376–1385; (*b*) S. Gaillard, X. Bantreil, A. M. Z. Slawin and S. P. Nolan, *Dalton Trans.*, 2009, 6967–6971.
23 M. Boronat, A. Corma, G. Arellano, M. Iglesias and F. Sanchez, *Organometallics*, 2010, **29**, 134–141.
24 M. L. Teyssot, A. S. Jarrousse, M. Manin, A. Chevry, S. Roche, F. Norre, C. Beaudoin, L. Morel, D. Boyer, R. Mahiou and A. Gautier, *Dalton Trans.*, 2009, 6894–6902.
25 J. Ratha, K. N. Majumdar, K. D. Saha and R. Bhadra, *Mol. Cell. Biochem.*, 2006, **290**, 113–123.
26 S. Mallick, B. C. Pal, J. R. Vedasiromoni, D. Kumar and K. D. Saha, *Cell. Physiol. Biochem.*, 2012, **30**, 915–926.
27 R. Uson, A. Laguna and M. Laguna, *Inorg. Synth.*, 1989, **26**, 85–91.
28 G. M. Sheldrick, *SHELX-97, Program for Crystal Structure Refinement*, University of Gottingen, Germany, 1997.
29 T. Mossman, *J. Immunol. Methods*, 1983, **65**, 55–63.